AGRICULTURAL AND FOREST METEOROLOGY

Supplementary Information for the Paper:

Carbon density in boreal forests responds non-linearly to temperature: an example from the Greater Khingan Mountains, northeast China

Yang Liu[a], Ralph Trancoso[b], Qin Ma[c], Philippe Ciais[d], Lidiane P. Gouvêa[e], Chaofang Yue[f], Jorge Assis[e, g], Juan A. Blanco[h]*

[a] College of Forestry, Inner Mongolia Agricultural University, Hohhot 010019, China
E-mail: liuyangvip@hotmail.com

[b] School of Biological Sciences, University of Queensland, Brisbane, Queensland 4072, Australia
E-mail: r.trancoso@uq.edu.au

[c] School of Geography, Nanjing Normal University, Nanjing 210023, China
Email: christine1511@gmail.com

[d] Laboratoire des Sciences du Climat et de l'Environnement, LSCE/IPSL, CEA-CNRS-UVSQ, Université Paris-Saclay, 91191 Gif-sur-Yvette, France
Email: philippe.ciais@lsce.ipsl.fr

[e] CCMAR - Centre of Marine Sciences, University of Algarve, Faro, Portugal
E-mail: lidi_pel@hotmail.com

[f] Forest Res Inst Baden Wurttemberg, Wonnhaldestr 4, D-79100 Freiburg, Germany
Email: ChaoFang.Yue@forst.bwl.de

[g] Faculty of Bioscience and Aquaculture, University of Nord, Bodø, Norway
E-mail: jorgemfa@gmail.com

[h] Departamento de Ciencias, Institute for Multidisciplinary Research in Applied Biology, Universidad Pública de Navarra, Campus de Arrosadía, Pamplona, Navarra, 31006, Spain
E-mail: juan.blanco@unavarra.es

Corresponding author: Juan A. Blanco
Departamento de Ciencias, Institute for Multidisciplinary Research in Applied Biology, Universidad Pública de Navarra, Campus de Arrosadía, Pamplona, Navarra, 31006, Spain
Tel: +34 948 169 859
Fax: +34 948 168 930
E-mail: juan.blanco@unavarra.es

Appendix 1. Additional information on tree species.

This appendix provides additional information on the equations and data used to estimate the carbon (C) content of forests in the Greater Khingan Mountains.

Estimation of C storage in trees (CS_{tree}) and its change

Currently, more than 70 variables are recorded for each PSP in the national forest inventory of the Greater Khingan Mountains. In each PSP, all trees with DBH ≥ 5 cm are identified by oil paint number, plates, and signs at the point of DBH, and newly recruited trees are tagged and measured. At the same time, variables such as the DBH, *H*, tree species, vitality status (live or dead), and polar coordinates are recorded for all trees with DBH ≥ 5 cm following a standard protocol (SFAPRC, 2011). Individual tree volumes for each PSP were estimated using a general volume table (see Supporting Information Table S1), then summed, and the result divided by the plot area to give the stand volume (m^3 ha^{-1}) for each census. That is, we calculated the stand-level volume/stand growing stock (*V*, m^3 ha^{-1}), which was based on repeated DBH measurements, by summing the volume of all trees within each sample plot for each census. The stand-level volume at each census includes the stem volumes of all living trees for all tree species with DBH ≥ 5 cm in this study. Thus, the stand-level volume included volume gain (positive) by the growth of surviving trees and ingrowth by newly recruited trees defined as the accretion of newly established trees of a certain size (the current DBH of trees ≥ 5 cm and previous DBH of trees < 5 cm in this study) in forest stands, and volume loss (negative) owing to tree mortality calculated as the volume sum of all dead trees between two consecutive inventory periods. The volume of dead trees still present at the PSP that were living in the previous inventory cycle is predicted in the same manner as for live trees (volume with time was composed of volume gain by the growth of surviving trees, ingrowth by newly recruited trees, and volume loss owing to tree mortality).

However, C storage in trees varies with forest types and age groups (Pan et al., 2004). First, we used the dominant species as the criterion to identify different forest types. The dominant species at each site was defined based on relative basal area or stem density for a specific tree species composition (when the DBH of trees does not attain the measurable diameter class, i.e., 5 cm in this study, tree species composition was calculated according to the stem density). The dominant species threshold with the highest relative basal area or stem density in a forest stand was identified as the dominant species. However, the tree species composition in the tree layer is relatively simple for the Greater Khingan Mountains; the main tree species comprise Dahurian larch (*Larix gmelinii* (Rupr.) Rupr.), white birch (*Betula platyphylla* Suk.), and aspen (*Populus davidiana* Dole). In this case, the dominant species threshold was defined as having >65% a certain tree species composition by stem density or basal area (SFAPRC, 2011).

Second, we determined the stand age considering two different scenarios. In the case of plantations, stand age is usually known from planting records. However, many native forests are uneven-aged forest stands. Stand age was determined as an arithmetic mean age of three average trees for the dominant species in the sample plot (Du et al., 2000) (the average tree is determined by the average DBH and the average height of the trees). The ages of the selected three average trees were estimated by counting growth rings based on increment cores taken from stems at 1.3 m height above the ground. As a result, the total biomass of trees was estimated in this study based on the volume-to-biomass method developed by Pan et al. (2004), which uses volume–biomass equations for forest types and age groups to convert timber volume to mass and account for non-commercial components (various tree components), including stems, branches, leaves, and roots. The forest biomass in trees was then converted to forest C storage based on a C concentration factor.

Estimation of C storage in understory and litter layers

To calculate C storage in the shrub layer (CS_{shrub}, Mg) for different forest age groups and types, a destructive harvesting method was used – aboveground biomass was cut and roots were excavated. The aboveground and belowground components were each weighed separately in the field in each quadrat (2 m × 2 m) of three quadrats along the diagonal of the field plot. All individual plants in each quadrat were collected and weighed. All samples were dried at 85 °C to constant weight. Approximately 30% of the dried sample in each quadrat was used to measure moisture content and C concentration by the potassium dichromate ($K_2Cr_2O_7$) oxidation method. The aboveground and belowground C storage in the shrub layer

was estimated by multiplying the dry biomass of the shrubs in each quadrat and the corresponding C concentration. We also calculated the C storage of the herbs (CS_{herb}, Mg) and litter (CS_{litter}, Mg) layers in three 1 m × 1 m quadrats in each plot for different forest age groups and types using the same method as for the shrub layer (herbs were also separated into aboveground and belowground components). The C storage in the understory and litter layers was estimated using Eqs. (4) to (6) listed in section 2.4 in the main text.

Estimation of total vegetation C storage

Total vegetation C storage was estimated with Eq. (8) listed in section 2.4 in the main text.

Change of C storage in vegetation

Carbon stored in the vegetation, including the tree, shrub, herb, and litter layers, of the Greater Khingan Mountains, northeast China was calculated based on the C storage in trees calculated from the national forest inventory data and the C storage in the shrub, herb, and litter layers based on the field measurements.

Change in C stored in trees, shrubs, herbs, litter, or vegetation in the Greater Khingan Mountains,

northeast China was estimated as follows with Eq. (S1):

$$CS_{change} = CS_t - CS_{t-n} \quad \text{(S1)}$$

where CS_{change} (Mg) is the change in C stored in trees, shrubs, herbs, litter, or vegetation in the Greater Khingan Mountains, northeast China, CS_t (Mg) is the C storage in trees, shrubs, herbs, litter, or vegetation in inventory t (at the end of the interval), CS_{t-n} (Mg) is the C storage in trees, shrubs, herbs, litter, or vegetation in inventory $t-n$ (at the beginning of the interval), and n is the number of years between inventories (n = 5 years in this study).

Annual increments in C storage illustrate the speed of tree growth processes in a certain period, and are a measure of change in C storage capacity of a stand over time (Liu et al., 2014). The annual increment of C storage in trees, shrubs, herbs, litter, or vegetation in the Greater Khingan Mountains, northeast China was calculated as follows with Eq. (S2) (Brown et al., 1988; Liu et al., 2014) for each interval period:

$$CSI_{annual} = (CS_t - CS_{t-n}) / n \quad \text{(S2)}$$

where CSI_{annual} (Tg C y^{-1}) is the annual increment in C storage in trees, shrubs, herbs, litter, or vegetation between the tth year and $t-$ nth year, and the other variables are as defined above.

The total biomass in trees was estimated in this study based on the volume-to-biomass method, which uses volume–biomass equations for forest types and age groups to convert timber volume to mass and account for non-commercial components (various tree components), such as branches, foliage, and roots. The forest biomass in trees (including aboveground and belowground biomass) was then converted to forest C storage based on a C concentration factor of 0.5.

Roots were excavated and aboveground biomass was measured in each quadrat of the shrub (2 m × 2 m) and herb (1 m × 1 m) layers to estimate C storage in shrubs and herb. The biomass of shrubs and herbs was considered to be split into two fractions: aboveground biomass and root biomass. Each fraction was analyzed in the laboratory for their C concentrations ([c] and [C]). Total shrub and herb C densities were calculated as aboveground biomass * aboveground [c] + root biomass * root [C].

Dominant species

The dominant species at each site were defined on the basis of relative basal area or stem density for a specific tree species composition. When the diameter at breast height (DBH, at 1.3 m above the ground) of trees was smaller than the measurable diameter class (5 cm in this study), tree species composition was calculated according to the stem density. The dominant species is usually defined as the one with the largest relative basal area or stem density in the forest stand. However, the tree species composition in the tree layer is relatively simple for forests in the

Greater Khingan Mountains, with the main species being Dahurian larch (*Larix gmelinii* (Rupr.) Rupr.), white birch (*Betula platyphylla* Suk.), and aspen (*Populus davidiana* Dole). In this case, the dominant species was defined as the one accounting for >65% of species composition based on stem density or basal area (SFAPRC, 2011).

Table S1. General volume equations used to estimate stand volume for the main tree species in forests in the Greater Khingan Mountains.

Volume	Tree species
$V = 0.000050168241\ D^{1.7582894}\ H^{1.1496653}$	*Larix gmelinii*
$V = 0.000054585749\ D^{1.9705412}\ H^{0.91418311}$	*P. sylvestris* var. *mongolica*
$V = 0.000051935163\ D^{1.8586884}\ H^{1.0038941}$	*Betula platyphylla*
$V = 0.000053474319\ D^{1.8778994}\ H^{0.99982785}$	*Populus davidiana* and *Populus suaveolens*
$V = 0.000052786451\ D^{1.7947313}\ H^{1.0712623}$	*Betula davurica*
$V = 0.000061125534\ D^{1.8810091}\ H^{0.94462565}$	*Quercus mongolica*
$V = 0.000041960698\ D^{1.9094595}\ H^{1.0413892}$	*Salix* and other tree species

Table S2. Forest age classifications for the main tree species in forests in the Greater Khingan Mountains.

Tree species	Forest origin	Forest age class				
		Young	Half mature	Near mature	Mature	Over mature
Picea	Natural	≤ 60	61-100	101-120	121-160	>161
	Planted	≤ 40	41-60	61-80	81-120	>121
Larix, *Abies*,	Natural	≤ 40	41-80	81-100	101-140	>141
Pinus sylvestris	Planted	≤ 20	21-30	31-40	41-60	>61
Populus, *Salix*,	Natural	≤ 20	21-30	31-40	41-60	>61
and other softwood	Planted	≤ 10	11-15	16-20	21-30	>31
Betula	Natural	≤ 30	31-50	51-60	61-80	>81
	Planted	≤ 20	21-30	31-40	41-60	>61
Quercus	Natural	≤ 40	41-60	61-80	81-120	>121
	Planted	≤ 20	21-40	41-50	51-70	>71

Note: Forest age class division followed the standardized methodology applied in Chinese forest inventories (SFAPRC, 2011). Unit of forest age is years.

Table S3. Parameters used to calculate forest biomass density (B, Mg ha^{-1}). Biomass density is expressed as a function of stand growing stock (V, m^3 ha^{-1}), $B = a + bV$, where a and b are constants for a forest type.

Forest type	Age group (years)	Volume range (m^3/ha)	*a*	*b*	R^2	Reference
Larix	≤ 40a	4 - 284	15.620	0.6589	0.8211	Pan, Luo,
	41 - 80a	4-611	31.878	0.6367	0.7924	Birdsey, Hom , &
	81 - 100a	69-411	15.857	0.6703	0.9003	Melillo (2004)
	101 - 140a	15-547	12.576	0.7406	0.9402	
	≥141a	50-792	-7.9247	0.7757	0.9403	
Pinus sylvestris var. *mongolica*	≤ 40a	8-130	18.967	0.6490	0.8078	Pan et al. (2004)
	41 - 100a	87-379	34.902	0.3927	0.5867	
	≥101a	198-500	22.470	0.3742	0.8375	
Abies and *Picea*	≤ 40a	6-273	13.210	0.7376	0.8605	Pan et al. (2004)
	41 - 80a	29-755	12.042	0.6317	0.8662	
	81 - 100a	54-933	41.312	0.4982	0.8238	
	101 - 140a	48-1235	48.690	0.4306	0.7913	
	≥141a	69-3831	39.201	0.4313	0.8557	
Quercus and other deciduous trees	≤ 40a	15-500	5.7107	0.9957	0.8578	Pan et al. (2004)
	41 - 60a	25-280	13.394	1.0564	0.8278	
	61 - 80a	33-304	24.774	0.8515	0.7246	
	≥81a	29-549	50.649	0.4829	0.6206	
Betula and *Populus*	≤ 10a	4-244	4.1318	0.8682	0.9060	Pan et al. (2004)
	11 - 15a	12-276	8.5271	0.8491	0.9056	
	16 - 20a	3-360	21.235	0.7594	0.8412	
	21 - 30a	9-652	36.308	0.6455	0.8434	
	≥31a	14-655	33.54	0.6642	0.8129	

Table S4. Carbon densities (Mg C ha^{-1}, mean ± standard deviation) of the shrub layer for different age classes of different forest types in the Greater Khingan Mountains.

Forest type	Age class				
	Young	Half mature	Near mature	Mature	Over mature
Larix gmelinii	1.42±0.10	2.46±0.59	0.86±0.17	0.88±0.03	0.73±0.12
P. sylvestris var. *mongolica*	1.10±0.22	1.42±0.18	0.83±0.14	1.35±0.06	1.26±0.30
Betula platyphylla	1.52±0.36	1.20±0.51	1.16±0.16	2.42±0.47	1.93±0.22
Populus davidiana	2.27±0.57	1.47±0.36	0.95±0.15	1.15±0.42	0.91±0.16
Quercus mongolica	1.41±0.31	0.53±0.05	0.12±0.01	0.22±0.03	0.15±0.22
Betula davurica	1.37±0.29	0.91±0.27	0.99±0.21	2.04±0.66	1.78±0.32
Populus suaveolens	1.89±0.41	1.11±0.34	0.72±0.32	0.92±0.25	0.81±0.24
Chosenia arbutifolia	1.37±0.31	0.88±0.11	0.69±0.16	0.66±0.14	0.60±0.04
Other forest types	1.22±0.25	0.71±0.14	0.56±0.16	0.52±0.19	0.46±0.18

Table S5. Carbon densities (Mg C ha^{-1}, mean ± standard deviation) of the herb layer for different age classes of different forest types in the Greater Khingan Mountains.

Forest type	Age class				
	Young	**Half mature**	**Near mature**	**Mature**	**Over mature**
Larix gmelinii	2.64±0.54	2.10±0.38	1.26±0.29	0.84±0.15	0.55±0.10
P. sylvestris var. *mongolica*	5.30±0.83	3.68±0.97	2.65±0.48	1.73±0.37	1.01±0.24
Betula platyphylla	4.28±1.11	4.16±0.66	2.88±0.45	1.97±0.26	0.84±0.29
Populus davidiana	3.94±0.57	3.66±0.75	2.55±0.54	2.99±0.64	1.83±0.47
Quercus mongolica	2.66±0.81	0.11±0.03	0.06±0.00	0.13±0.03	0.04±0.00
Betula davurica	3.17±1.09	2.97±0.86	1.86±0.66	1.07±0.26	0.59±0.15
Populus suaveolens	3.01±0.82	2.77±0.91	2.04±0.77	1.63±0.34	1.18±0.40
Chosenia arbutifolia	2.91±0.91	2.64±0.83	1.39±0.47	0.97±0.11	0.43±0.13
Other forest types	2.55±0.96	2.17±0.31	1.11±0.24	0.73±0.19	0.32±0.08

Table S6. Carbon densities (Mg C ha^{-1}, mean ± standard deviation) of the litter layer for different age classes of different forest types in the Greater Khingan Mountains.

Forest type	Age class				
	Young	**Half mature**	**Near mature**	**Mature**	**Over mature**
Larix gmelinii	0.81±0.05	1.39±0.15	3.14±0.84	3.47±1.34	3.70±1.26
P. sylvestris var. *mongolica*	0.75±0.12	1.36±0.27	1.42±0.52	3.29±0.54	3.49±1.22
Betula platyphylla	0.53±0.02	0.93±0.15	1.24±0.31	1.70±0.29	1.99±0.46
Populus davidiana	1.96±0.38	1.73±0.47	0.59±0.09	0.67±0.24	0.75±0.14
Quercus mongolica	1.19±0.21	0.78±0.08	0.48±0.07	0.59±0.03	0.68±018
Betula davurica	0.47±0.13	0.63±0.18	0.87±0.18	1.02±0.27	1.33±0.41
Populus suaveolens	1.68±0.29	1.40±0.37	0.39±0.13	0.44±0.15	0.61±0.21
Chosenia arbutifolia	0.43±0.11	0.56±0.13	0.66±0.09	0.84±0.23	0.91±0.32
Other forest types	0.38±0.12	0.48±0.14	0.53±0.18	0.69±0.14	0.77±0.16

Appendix 2. Number of field plots required for systematic random sampling in the Greater Khingan Mountains

The number of field plots (*N*) required for systematic random sampling was determined, taking into account the inherent variability of the attribute values (volume was used in this study) of the population, the degree of precision required for the results, and the confidence coefficient applied to confidence intervals of sample estimates (Köhl, Magnussen, & Marchetti, 2006). The formula used to determine the *N* for systematic random sampling was as follows:

$$N = \left(\frac{t_{n-1,\alpha} \cdot C}{E} \right)^2 \quad \text{(S3)}$$

where $t_{n-1,\alpha}$, which is the αth quantile of student's *t* distribution, depends on the degrees of freedom and can be obtained from the *t* distribution table for a small sample size. For large sample sizes, say, larger than 30, the quantiles of the *t* distribution are very close to the corresponding quantiles of a standard normal distribution u_α (u_α = 1.96) (Köhl et al., 2006), *E* is the relative error limit, and *C* is the coefficient of variation. Provided that an estimate of the maximum and minimum values of the population units can be obtained, the coefficient of variation (*C*) (Song & Li, 2007), which is approximately estimated by an empirical formula, can be calculated as follows:

$$C = \left(y_{max} - y_{min} \right) / 6\bar{y} \quad \text{(S4)}$$

where y_{max} is the maximum value of the population units, y_{min} is the minimum value of the population units, and $\bar{y}$ is the mean value of the population units.

The results of the field surveys showed that the maximum volume, minimum volume, and mean volume were 180.4 m^3/ha, 10.6 m^3/ha, and 96.7 m^3/ha in forests of the Greater Khingan Mountains, respectively. The estimation accuracy (*P*) was generally not less than 95% (*E* = 1-*P* = 5%) and typically the 95% confidence interval is presented (α=0.05). These values were substituted into Eqs. (S3) and (S4). On the basis of these calculations, the minimum *N* was 132 for systematic random sampling in the Greater Khingan Mountains to estimate the regional C density and to examine the potential drivers of forest ecosystem C changes.

Appendix 3. Quality evaluation of gridded soil carbon data

We compiled measured data from 48 field-based soil studies from the same locations in the Greater Khingan Mountains (Figure S1 and Table S7). Then, we used the nonparametric Wilcoxon rank sum test for paired data or a paired t-test to detect statistical differences between actual soil measurements ("local" data) and gridded values of soil organic carbon density (SOCD) extracted from the WISE30sec dataset for the same geographical coordinates. As a result, we obtained 48 paired sites with SOCD, meeting the requirement of a sufficiently large sample size (30 or more, (Karandinos, 1976; Song & Li, 2007). The normality and homogeneity of variances were tested using Shapiro–Wilk's and Bartlett's tests ($p < 0.05$). The Wilcoxon rank-sum test, which is a nonparametric two-sample test, was used to compare differences between two data sources when the SOCD data were not normally distributed ($p< 0.05$). The results showed that there were no significant differences between the field and gridded data collections (p=0.126 >0.05). The correlation coefficients between data sources were acceptably high (0.76) given the uncertainties associated with each dataset. Hence, we considered that using the gridded dataset from the WISE30sec database was an acceptable substitute for direct soil analyses, which unfortunately were not included as part of the Chinese national forest inventory measurements.

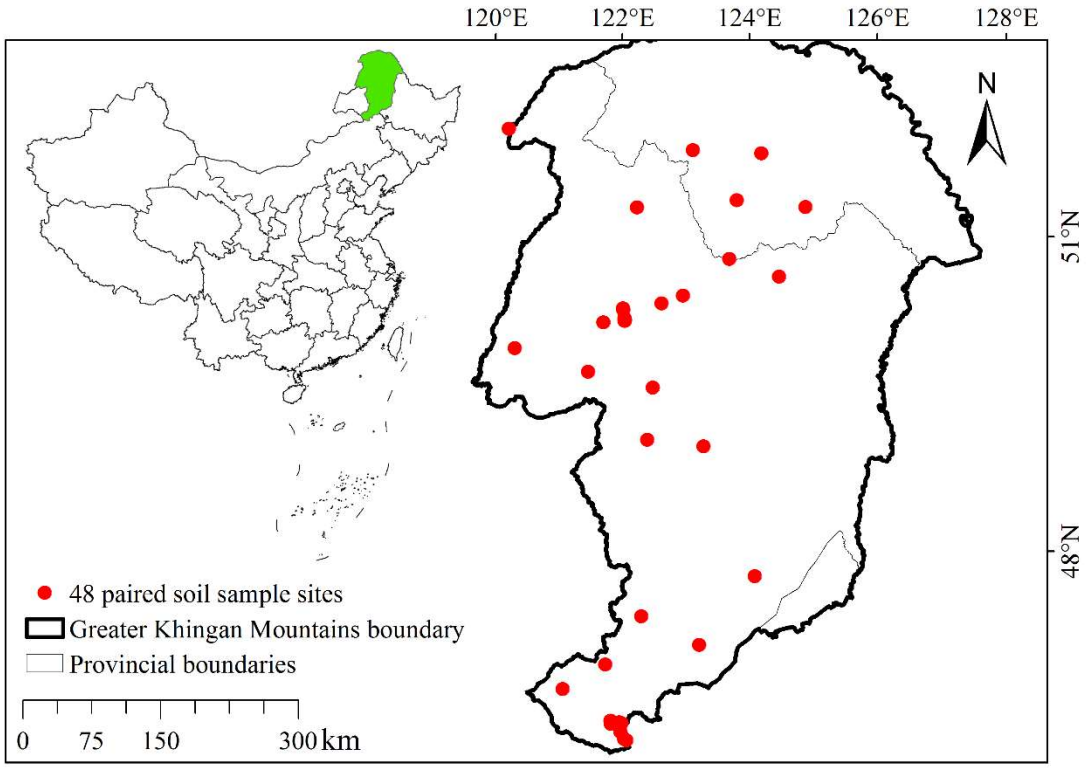

Figure S1. Location of 48 paired soil sample sites across the Greater Khingan Mountains, northeast China. Some dots overlap each other and are thus not visible.

Table S7. List of previous studies used to evaluate the quality of the gridded soil carbon data.

Code	Long.	Lat.	SOCD (Mg C ha^{-1})	Method	Time	Type of data	Reference	Bulk density (kg dm^{-3})	SOC (g C kg^{-1})	Coarse fragments >2mm (vol%)	SOCD generated by WISE30sec (Mg C ha^{-1})
Soil1	121.5105	50.8400	50.10	Direct	2007-2008	Literature data	Hai (2009)	1.48	15.99	7	44.02
Soil2	121.5124	50.8300	50.11	Direct	2007-2009	Literature data	Hai (2009)	1.48	15.99	7	44.02
Soil3	121.5097	50.8300	60.90	Direct	2007-2010	Literature data	Hai (2009)	1.48	15.99	7	44.02
Soil4	121.5032	50.8200	65.27	Direct	2007-2011	Literature data	Hai (2009)	1.48	15.99	7	44.02
Soil5	121.5089	50.8400	134.84	Direct	2007-2012	Literature data	Hai (2009)	1.11	65.69	1	144.37
Soil6	124.4829	51.6710	126.40	Indirect	2010	Literature data	Huang (2011)	1.11	65.69	1	144.37
Soil7	123.4500	51.8300	69.92	Direct	2009	Literature data	Qi (2011)	1.48	15.99	7	44.02
Soil8	123.2100	51.2800	72.39	Direct	2009	Literature data	Qi (2011)	1.48	15.99	7	44.02
Soil9	123.9300	52.2400	114.93	Direct	2009	Literature data	Qi (2011)	1.32	22.44	2	58.06
Soil10	122.8800	52.3600	106.52	Direct	2009	Literature data	Qi et al. (2013)	1.11	65.69	1	144.37
Soil11	121.5102	50.8441	59.70	Direct	2010-2012	Literature data	Wang (2013)	1.48	15.99	7	44.02
Soil12	121.5100	50.8200	70.15	Direct	2010-2012	Literature data	Wang (2013)	1.48	15.99	7	44.02
Soil13	120.6270	46.9733	26.36	Direct	2013	Experimental data	Xu, He , & Yu (2020)	1.48	15.99	7	44.02
Soil14	120.7662	46.9375	38.87	Direct	2013	Experimental data	Xu et al. (2020)	1.48	15.99	7	44.02
Soil15	120.7675	46.9372	40.51	Direct	2013	Experimental data	Xu et al. (2020)	1.24	25.73	15	54.24
Soil16	120.7928	46.7781	41.26	Direct	2013	Experimental data	Xu et al. (2020)	1.48	15.99	7	44.02
Soil17	120.6283	46.9725	43.47	Direct	2013	Experimental data	Xu et al. (2020)	1.48	15.99	7	44.02
Soil18	120.7668	46.9378	44.82	Direct	2013	Experimental data	Xu et al. (2020)	1.24	25.73	15	54.24
Soil19	120.6273	46.9405	48.74	Direct	2013	Experimental data	Xu et al. (2020)	1.48	15.99	7	44.02
Soil20	120.7647	46.9348	49.55	Direct	2013	Experimental data	Xu et al. (2020)	1.48	15.99	7	44.02
Soil21	120.6560	46.9540	60.55	Direct	2013	Experimental data	Xu et al. (2020)	1.48	15.99	7	44.02
Soil22	120.7518	46.8535	65.35	Direct	2013	Experimental data	Xu et al. (2020)	1.48	20.6	5	57.93
Soil23	120.7777	46.9365	67.77	Direct	2013	Experimental data	Xu et al. (2020)	1.24	25.73	15	54.24

Table S7. Cont.

Soil24	120.6540	46.9546	68.15	Direct	2013	Experimental data	Xu et al. (2020)	1.48	15.99	7	44.02
Soil25	120.8196	46.7640	72.19	Direct	2013	Experimental data	Xu et al. (2020)	1.48	15.99	7	44.02
Soil26	120.7701	46.9398	75.45	Direct	2013	Experimental data	Xu et al. (2020)	1.24	25.73	15	54.24
Soil27	120.6532	46.9559	77.25	Direct	2013	Experimental data	Xu et al. (2020)	1.48	15.99	7	44.02
Soil28	120.7475	46.9479	78.27	Direct	2013	Experimental data	Xu et al. (2020)	1.48	15.99	7	44.02
Soil29	120.7332	46.9078	78.83	Direct	2013	Experimental data	Xu et al. (2020)	1.48	15.99	7	44.02
Soil30	122.9517	48.2030	33.27	Direct	2017	Experimental data	This study	1.29	32.28	15	70.79
Soil31	121.9024	51.8862	109.21	Direct	2017	Experimental data	This study	1.11	65.69	1	144.37
Soil32	122.4485	49.5209	11.31	Direct	2017	Experimental data	This study	1.48	15.99	7	44.02
Soil33	123.9258	51.0470	116.61	Direct	2017	Experimental data	This study	1.11	65.69	1	144.37
Soil34	121.8085	50.1454	31.39	Direct	2017	Experimental data	This study	1.28	23.34	1	59.15
Soil35	120.6427	47.5263	29.23	Direct	2017	Experimental data	This study	1.24	25.73	15	54.24
Soil36	119.9947	47.3310	54.78	Direct	2017	Experimental data	This study	1.29	32.28	15	70.79
Soil37	121.1850	50.8286	31.73	Direct	2017	Experimental data	This study	1.48	15.99	7	44.02
Soil38	121.5053	50.9397	32.49	Direct	2017	Experimental data	This study	1.48	15.99	7	44.02
Soil39	119.8033	50.6746	57.35	Direct	2017	Experimental data	This study	1.48	20.6	5	57.93
Soil40	122.0220	47.6090	56.62	Direct	2017	Experimental data	This study	1.24	25.73	15	54.24
Soil41	122.4331	50.9903	55.49	Direct	2017	Experimental data	This study	1.48	15.99	7	44.02
Soil42	121.9034	51.8868	55.78	Direct	2017	Experimental data	This study	1.48	15.99	7	44.02
Soil43	121.5056	50.9233	57.85	Direct	2017	Experimental data	This study	1.48	15.99	7	44.02
Soil44	121.6310	49.6524	60.86	Direct	2017	Experimental data	This study	1.48	15.99	7	44.02
Soil45	120.8675	50.3724	79.75	Direct	2017	Experimental data	This study	1.28	23.34	1	59.15
Soil46	121.2396	47.9531	169.84	Direct	2017	Experimental data	This study	1.11	65.69	1	144.37
Soil47	120.0591	52.7695	103.79	Direct	2017	Experimental data	This study	1.27	38.09	21	76.43
Soil48	122.0936	50.9419	73.09	Direct	2017	Experimental data	This study	1.48	15.99	7	44.02

Notes:

Soil organic carbon density (SOCD, Mg C ha^{-1}) in 0–20 cm soil layer at the sampled sites.

Field-measured data from papers published from 2007 to 2013 or obtained in this study.

Appendix 4. Data sources and extended results of relationships between total C density and environmental variables.

Management and disturbance detection

Disturbance events were determined using the remote-sensing derived delta Normalized Burn Ratio (dNBR) method. The dNBR is widely used to detect disturbances and their severity in various forest ecosystems (Miller & Thode, 2007; Miller et al., 2009), and has been proven to be applicable to our study area (Fang & Yang, 2014). The dNBR images were calculated as the difference in NBR values between the year before and the year after the disturbance. Larger positive dNBR values indicate more severe disturbance events. The dNBR was computed as follows:

$$NBR = \frac{\rho NIR - \rho SWIR2}{\rho NIR + \rho SWIR2} \quad \text{(S5)}$$

$$dNBR = NBR_{year-1} - NBR_{year+1} \quad \text{(S6)}$$

where ρNIR is the reflectance in the near infrared band (e.g., Landsat TM/ETM+ band 4, 0.76–0.90 μm) and $\rho SWIR2$ is the reflectance in the short-wavelength infrared region (SWIR) (e.g., Landsat TM/ETM+ band 7, 2.08–2.35 μm).

We used all the Landsat images available during peak growing seasons (July and August) to calculate NBR images. To do so, we first calculated the annual reflectance for each Landsat band using the maximum value composite approach. Clouds, cloud shadows, snow, and water were masked out using Fmask algorithms (Zhu & Woodcock, 2012). The dNBR image for each year was calculated using the equations mentioned above. Lastly, we sampled the dNBR value for each sampling point. This process was performed using the Google Earth Engine platform.

A dNBR value greater than 100 indicated a disturbance event, and the magnitude of the value was an indicator of disturbance severity. We did not differentiate disturbance types (e.g., timber harvest and fire) because it required additional data that were not available.

Stand age

In the case of plantations, stand age is usually known from planting records. However, many native forests are uneven-aged forest stands. For those forests, stand age was determined as an arithmetic mean age of three average trees of the dominant species in the sample plot (Du, Tang, & Wang, 2000) (an “average” tree was determined by the average diameter at breast height and the average tree height). The ages of the selected three average trees were estimated by counting

growth rings based on increment cores taken from stems at a height of 1.3 m above the ground.

Forest type

The forests in the Greater Khingan Mountains were grouped into the following three types according to the International Geosphere-Biosphere Programme (IGBP) land cover classification (Loveland & Belward, 1997; Belward, Estes, & Kline, 1999): deciduous needleleaf forests (dominated by deciduous needleleaf (larch) trees; canopy > 2 m; tree cover >60%); deciduous broadleaf forests (dominated by deciduous broadleaf trees; canopy > 2 m; tree cover >60%); and mixed forests (dominated by neither deciduous nor evergreen (40%–60% of each) tree type (canopy > 2 m); tree cover >60%).

Table S8. Spatial resolution, data type, source and reference for 19 ancillary variables used in the boosted regression trees (BRT) model.

Variable	Spatial resolution (degrees)	Type	Source	Reference
MAP	30 seconds	Climate	WorldClim	https://www.worldclim.org
MAT	30 seconds	Climate	WorldClim	
SR	30 seconds	Climate	WorldClim	
BIO4	30 seconds	Climate	WorldClim	
BIO15	30 seconds	Climate	WorldClim	
BIO18	30 seconds	Climate	WorldClim	
Elev	30 seconds	Elevation	WorldClim	https://www.worldclim.org
AI	30 seconds	Climate	Global-Aridity_ET0	https://doi.org/10.6084/m9.figshare.7504448.v3
ET0	30 seconds	Climate	Global-ET0	
CWD	2.5 minutes	Climate	Chave	http://chave.ups-tlse.fr/pantropical_allometry.htm
CLPC	30 seconds	Soil	WISE30sec	http://www.isric.org
PH	30 seconds	Soil	WISE30sec	
SC	30 seconds	Soil	WISE30sec	
TP	30 seconds	Soil	WISE30sec	
TN	30 seconds	Soil	WISE30sec	
H'	-	Biodiversity	Filed survey	See Methods
AGE	-	Stand age	Filed survey	See Appendix 4
Forest type	-	Forest type	IGBP	See Appendix 4
Disturb	30 meters	Management and disturbance	Landsat imagery	See Appendix 4

Notes: MAP: mean annual precipitation (mm), MAT: mean annual temperature (°C), SR: solar radiation (kJ m^{-2} day^{-1}), BIO4: temperature seasonality (°C), BIO15: precipitation seasonality (mm), BIO18: precipitation of warmest quarter (mm), Elev: elevation (m), AI: aridity index, ET0: potential evapo-transpiration (mm day^{-1}), CWD: climatic water deficit (mm yr^{-1}), CLPC: clay content (mass %), PH: soil pH measured in water, SC: sand content (mass %), TP: total phosphorus (g kg^{-1}), TN: total nitrogen (g kg^{-1}), *H*': Shannon-Wiener diversity index, AGE: stand age, Disturb: management and disturbance identified using the delta Normalized Burn Ratio (dNBR).

Table S9. Interactions between variables obtained in the model.

Variable 1	Variable 2	Interaction (%)
CLPC	MAT	0.18
	MAP	0.01
	PH	0.02
PH	MAT	0.02
BIO 15	PH	0.01

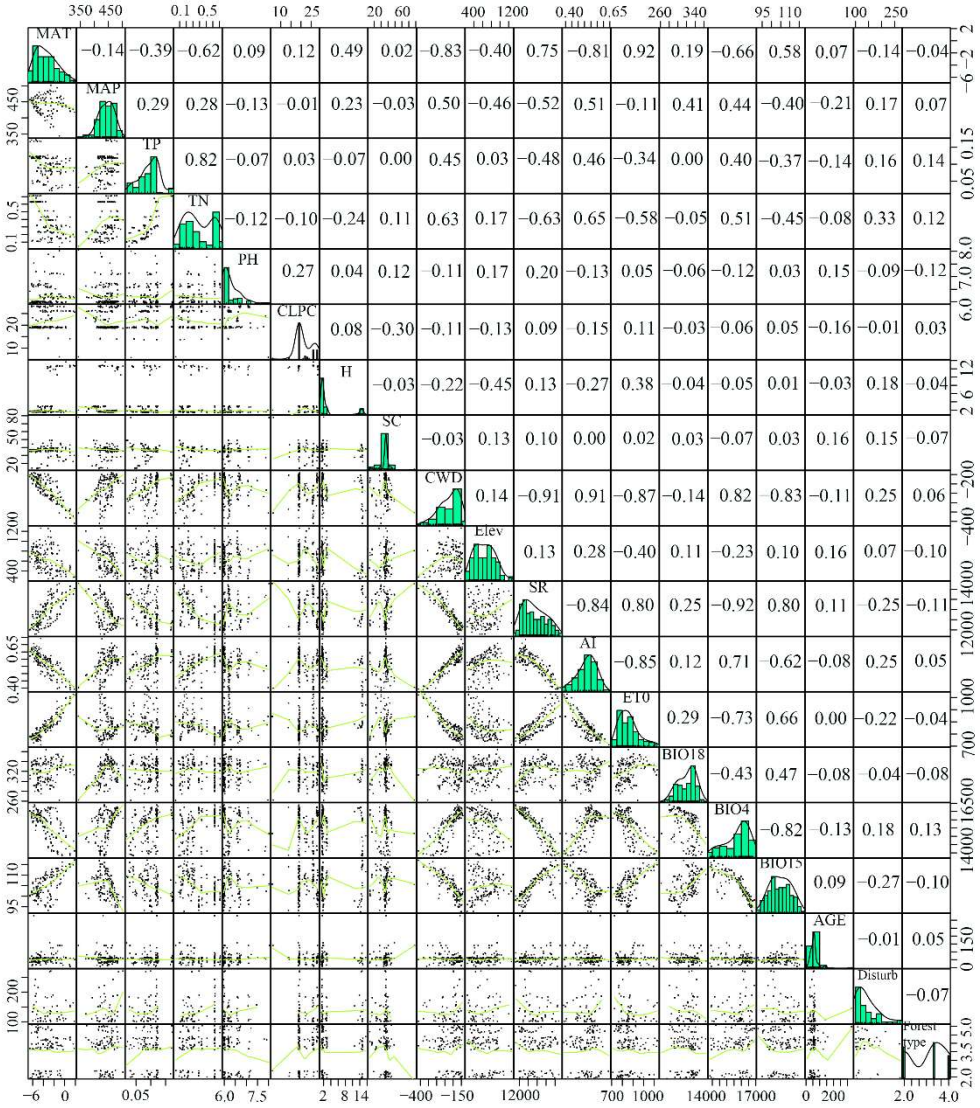

Figure S2. Histogram and pair plots of variables used in modeling of the boreal forests. Numbers indicate correlations between pairs of variables.

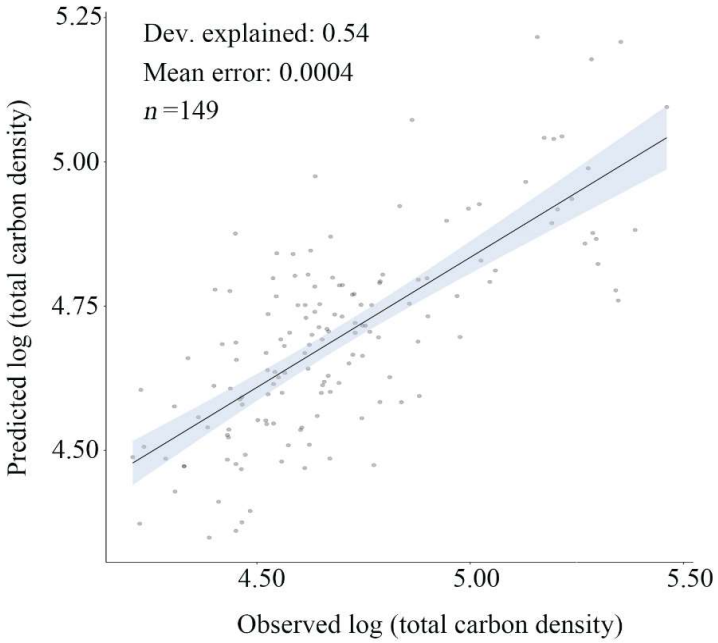

Figure S3. Relationship between observed and predicted total carbon (C) density of boreal forests (deviance explained: 0.54, *n*=149).

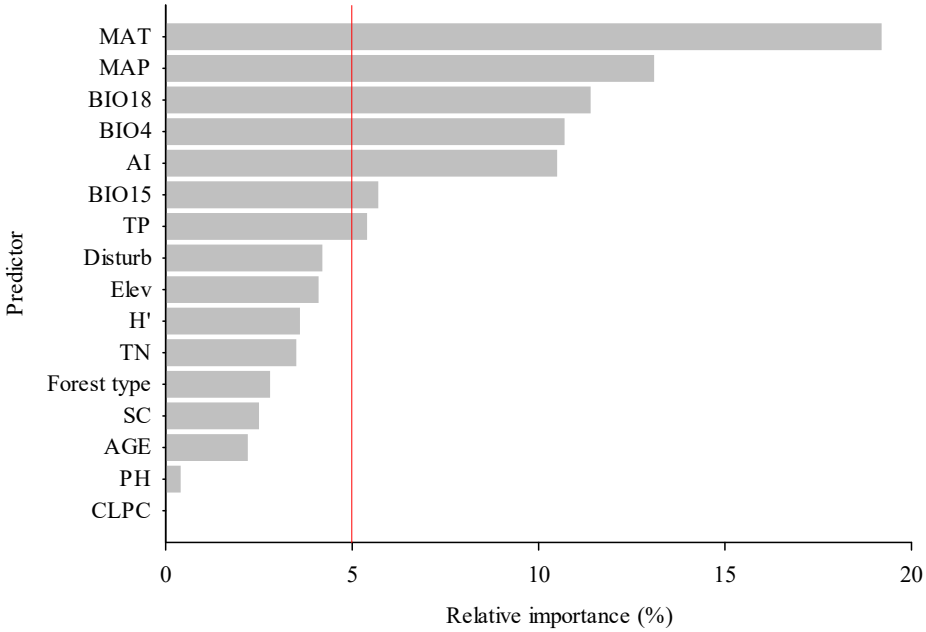

Figure S4. Relative importance (%) of all variables for the model of total carbon (C) density of forest ecosystems (including forest vegetation and soil C density, Mg C ha^{-1}) with mean annual temperature (MAT; °C), mean annual precipitation (MAP; mm), precipitation of warmest quarter (BIO18; mm), temperature seasonality (BIO4; °C), aridity index (AI), precipitation seasonality (BIO15; mm), total phosphorus (TP; g kg^{-1}), management and disturbance (Disturb), elevation (Elev; m), Shannon-Wiener diversity index (*H'*), total nitrogen (TN, g kg^{-1}), forest type, sand content (SC, mass %), stand age (AGE, year), pH (soil) and clay content (CLPC; mass %). Red line indicates 5% contribution to the model.

Appendix 5. Additional information on quantile regression.

Quantile regression (QR), first developed by Koenker & Bassett (1978), was a breakthrough in statistics and has a wide range of applications. The QR method provides a modeling framework for estimating conditional quantiles of the response variable. Each QR characterizes a specific (center or tail) point of a conditional distribution. Thus, combining different QRs provides a more complete description of the underlying conditional distribution. QR has an advantage over ordinary least-squares regression when the conditional distribution is not standard, such as in cases of non-normal behavior, heavy-tailed distributions, and outliers. Preliminary analyses revealed a strong nonlinear and nonstandard relationship between the total C density and MAT. QR overcomes the shortcomings of this relationship and estimates a more accurate quantitative relationship between the total C density and MAT.

The basic theory of the QR analysis model is as follows. Let Y be a response variable and $X \in \mathrm{R}^p$ be the covariates. Then, the τ th conditional quantile of Y is defined as $Q_\tau(Y \mid X) = \inf\{y \in \mathrm{R}, F_{Y|X}(y) \geq \tau\}$, where $\tau \in (0,1)$ and $F_{Y|X}(y)$ is the conditional distribution of Y given X. The conditional quantile $Q_\tau(Y \mid X)$ is a solution to

$$Q_\tau(Y \mid X) = \arg\min_g E[\rho_\tau(Y - g(x)) \mid X], \qquad \text{(S7)}$$

where $\rho_\tau(u) = u(\tau - I(u < 0))$ is the quantile loss or pinball loss, and $I(\cdot)$ is the indicator function. The theory of the QR method was comprehensively discussed by Koenker (2005).

In practice, the function form of $Q_\tau(Y \mid X)$ can be a parametric or nonparametric model, but the latter makes fewer assumptions and is more flexible and robust than the former. In this case, we used the nonparametric model to determine the effect of MAT on the total C density because loose assumptions are made about the distribution of the error term that the nonparametric model predicts (Belaïd, Youssef, & Lazaric, 2020). Many nonparametric QR models, such as local polynomial and smoothing spline methods, have been introduced in the literature (Yu, Lu, & Stander, 2003). Among them, the smoothing splines quantile regression model using the total variation roughness penalty method described by Koenker, Ng , & Portnoy (1994) is attractive for its simplicity and interpretability.

Specifically, $g_\tau(x)$ denotes the τ conditional quantile function of the total C density for a given x (MAT). Koenker et al. (1994) suggested minimizing the roughness penalty problem

$$R_{\tau,\lambda}(g) = \sum_i^n \rho_\tau(y_i - g(x_i)) + \lambda \int_{-\infty}^{+\infty} | g''(x) | \mathrm{d}x, \qquad \text{(S8)}$$

where λ is the smoothing parameter or penalty parameter, y_i is the total C density, and x_i is the associated MAT, with $i = 1, 2, \ldots, n$. Under some assumptions, the solution $\hat{g}_\tau(x)$ of the above minimization problem is a linear spline with knots at x_i. The quantile curve obtained using this method offers a simple and direct approach to estimate univariate change-point models for piecewise-linear continuous functions.

In this study, the QR was implemented in the R package quantreg (Koenker, 2018). The smoothing parameter (λ) was selected by minimizing the Schwarz information criterion as suggested by Koenker et al. (1994).

Table S10. QR results for the total C density.

τ	λ (Smoothing parameter)	*F* value	MAT_0 (Inflection point)	β_1	β_2
0.1	3.80	1700***	-2.1	2.0	-1.4
0.25	2.89	1043***	-2.1	2.7	-2.4
0.5	5.60	4843***	-2.4	3.7	-2.8
0.75	1.90	1504***	-4.5	3.2	-6.4
0.9	3.12	24930***	-3.6	0.3	-15.7

Note: β_1 and β_2 are slopes of the estimated piecewise-linear quantile curves. *F*-value indicates the significance of non-parametric components (i.e., *qss* terms). *** indicates a significance level of 0.01.

Appendix 6. Additional information on ANOVA of carbon storage or density among different components of forest vegetation, age classes, and forest types

Table S11. Area, carbon (C) storage, C density, and change in C storage in trees, shrubs, herbs, litter, and forest vegetation in the Greater Khingan Mountains, China from 1999 to 2018

Vegetation type	Period	Area (10^6 ha)	C storage (Tg C)	C density (Mg C ha^{-1})	C storage change (Tg C y^{-1})	Growth rate (%)
Tree	1999–2003	14.55	565.33	38.86		
	2004–2008	14.77	591.89	40.07	5.31	0.94
	2009–2013	14.89	619.07	41.57	5.44	0.92
	2014–2018	15.16	652.22	43.04	6.63	1.07
Shrub	1999–2003	14.55	22.41	1.54		
	2004–2008	14.77	24.18	1.64	0.35	1.58
	2009–2013	14.89	24.25	1.63	0.01	0.06
	2014–2018	15.16	24.75	1.63	0.10	0.41
Herb	1999–2003	14.55	38.59	2.65		
	2004–2008	14.77	41.92	2.84	0.67	1.72
	2009–2013	14.89	42.40	2.85	0.10	0.23
	2014–2018	15.16	43.19	2.85	0.16	0.37
Litterfall	1999–2003	14.55	21.58	1.48		
	2004–2008	14.77	19.31	1.31	-0.45	-2.11
	2009–2013	14.89	19.59	1.32	0.06	0.29
	2014–2018	15.16	19.98	1.32	0.08	0.39
Total	1999–2003	14.55	647.91	44.54		
	2004–2008	14.77	677.30	45.85	5.88	0.91
	2009–2013	14.89	705.31	47.36	5.60	0.83
	2014–2018	15.16	740.13	48.84	6.96	0.99

Table S12. ANOVA of carbon storage (Tg, mean ± standard error) in different components of forest vegetation (tree, shrub, herb, and litter) during the monitoring period.

Carbon storage				Number of samples	*F*	*p*
Tree	Shrub	Herb	Litter			
607.13±18.61[a]	23.90±0.51[b]	41.53±1.01[b]	20.12±0.51[b]	4	963.6	0.000

Note: Different superscript letters in the same row indicate significant differences among components; same superscript letter in the same row indicates no significant differences among components (Tukey's HSD, $p < 0.05$).

Table S13. ANOVA of carbon density (Mg C ha^{-1}, mean ± standard error) in different components of forest vegetation (tree, shrub, herb, and litter) during the monitoring period.

Carbon density				Number of samples	*F*	*p*
Tree	Shrub	Herb	Litter			
40.89±0.91[a]	1.61±0.02[b]	2.80±0.05[b]	1.36±0.04[b]	4	1835.8	0.000

Note: Different superscript letters in the same row indicate significant differences among components; same superscript letter in the same row indicates no significant differences among components (Tukey's HSD, $p < 0.05$).

Table S14. ANOVA of carbon storage (Tg, mean ± standard error) for different tree age classes (young, half mature, near mature, mature, and over mature forests) during the monitoring period.

Carbon storage					Number of samples	*F*	*p*
Young	Half mature	Near mature	Mature	Over mature			
108.49±5.08[a]	433.31±26.10[b]	70.59±3.19[a]	68.90±8.31[a]	11.37±2.12[c]	4	179.3	0.000

Note: Different superscript letters in the same row indicate significant differences among age classes; same superscript letter in the same row indicates no significant differences among age classes (Tukey's HSD, $p < 0.05$).

Table S15. ANOVA of carbon density (Mg C ha^{-1}, mean ± standard error) for different tree age classes (young, half mature, near mature, mature, and over mature forests) during the monitoring period.

Carbon density					Number of samples	*F*	*p*
Young	Half mature	Near mature	Mature	Over mature			
29.29±1.99[a]	52.69±0.32[b]	51.33±0.38[b]	53.53±0.70[b]	49.41±1.19[b]	4	84.3	0.000

Note: Different superscript letters in the same row indicate significant differences among age classes; same superscript letter in the same row indicates no significant differences among age classes (Tukey's HSD, $p < 0.05$).

Table S16. ANOVA of carbon density (Mg C ha^{-1}, mean ± standard error) for different forest types during the monitoring period.

Forest type	Carbon density
Larix gmelinii	47.52±0.95[a]
P. sylvestris var. *mongolica*	50.52±0.26[ab]
Betula platyphylla	45.48±0.64[a]
Populus davidiana	58.37±1.73[c]
Quercus mongolica	37.21±2.34[d]
Betula davurica	26.06±1.86[e]
Populus suaveolens	57.89±0.17[cg]
Chosenia arbutifolia	42.87±1.94[adf]
Other forest types	31.49±0.34[de]
Number of samples	4
F	64.2
p	0.000

Note: Different superscript letters in the same column indicate significant differences among forest types; same superscript letter in the same column indicates no significant differences among forest types (Tukey's HSD, $p < 0.05$).

Appendix 7. Additional information on determining a quantitative relationship between other covariates and total C density in forest ecosystems across the Greater Khingan Mountains

We specifically included six additional predictors (mean annual precipitation (MAP; mm), precipitation of warmest quarter (BIO18; mm), temperature seasonality (BIO4; °C), aridity index (AI), precipitation seasonality (BIO15; mm) and total phosphorus (TP; g kg^{-1})) to take into account other factors that may affect total C density. Theses six predictors were selected by boosted regression trees (BRT) modelling (the predictors with individual contributions of >5% and a combined contribution of 56.9% to total C density (Figures 5 and S4)). Next, regression analyses were conducted to explore the quantitative relationships between total C density and these six additional predictors. The results showed that the spatial pattern of the total C density was strongly correlated with the MAP, BIO18, and BIO4 ($R^2 = 0.30 - 0.42$, $p < 0.05$, Figure S5). In forest ecosystems, the total C density decreased with increasing precipitation (MAP and BIO18) but decreased at a faster rate in the regions with increasing BIO18 than in those with increasing MAP (total C density in forest ecosystems was more strongly negatively correlated with BIO18 than with MAP) (3.3 Mg C ha^{-1}/10 mm *vs.* 2.5 Mg C ha^{-1}/10 mm, Figure S5 (a and b)). By contrast, the total C density was positively correlated with BIO4. In this case, when BIO4 increased by 1°C, the total C density of forest ecosystems increased by 0.1 Mg C ha^{-1} (Figure S5 (c)). These results suggested that total C density of forest ecosystems exhibited various feedbacks to climate variables/conditions. However, there was no significant relationship, or a weak relationship, between total C density and AI, BIO15, and TP ($R^2 < 0.1$, $p > 0.05$; Figure S5 (d, e and f)), indicating that each of these variables/parameters made a relatively small contribution to total C density. These small contributions were also verified through the BRT modelling (as shown in Figures 5 and S4).

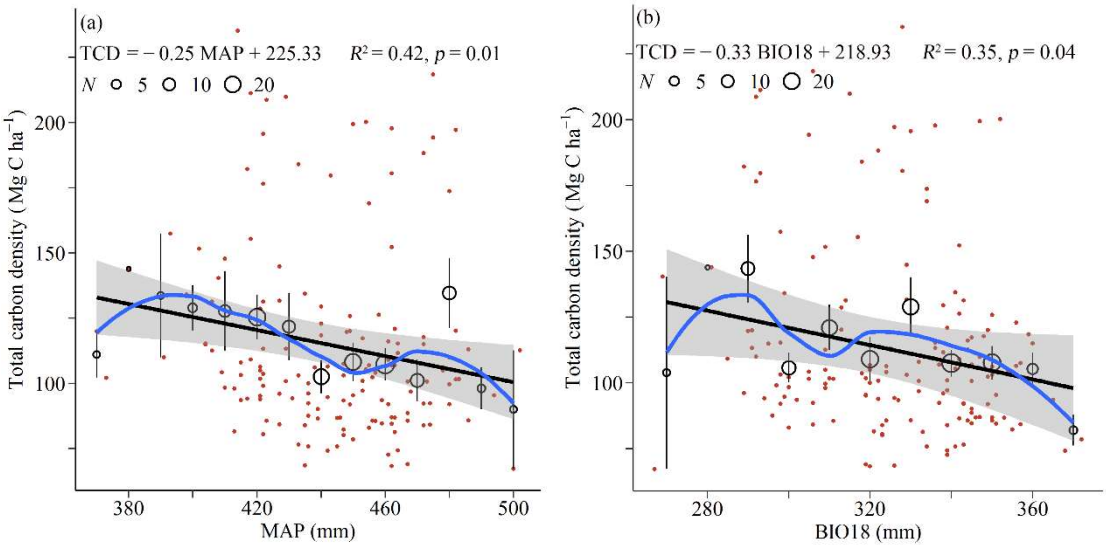

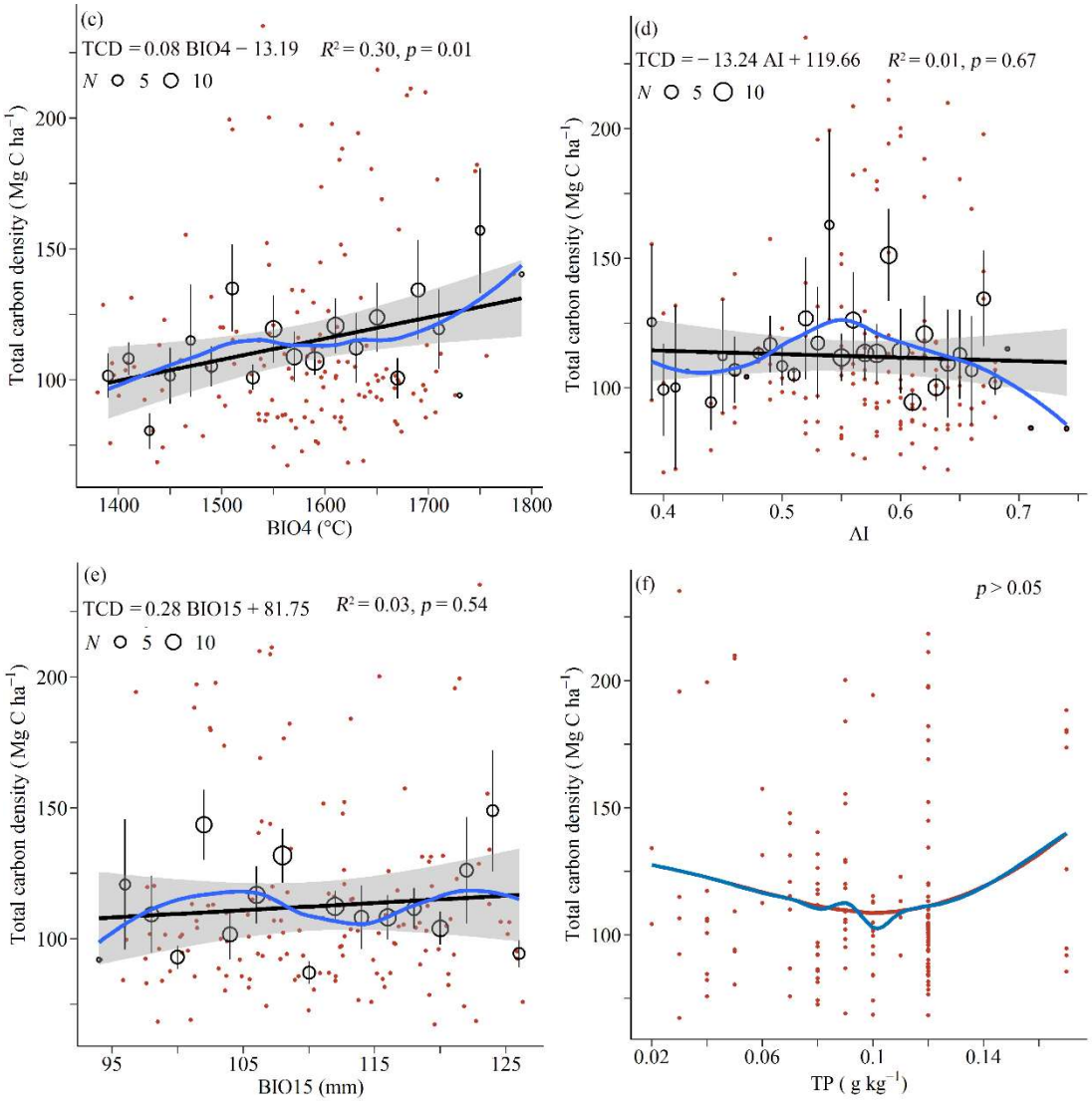

Figure S5. Relationships between total carbon (C) density of forest ecosystems (including forest vegetation and soil C density, Mg C ha^{-1}) and (a) mean annual precipitation (MAP; mm), (b) precipitation of warmest quarter (BIO18; mm), (c) temperature seasonality (BIO4; °C), (d) aridity index (AI), (e) precipitation seasonality (BIO15; mm), and (f) total phosphorus (TP; g kg^{-1}) (factors with contributions of >5% to model of total C density in the Greater Khingan Mountains. Black circles and error bars indicate mean total C density and standard errors for each 10 mm, 10 mm, 20 °C, 0.01 (not grouped), 2 mm, and 0.01 g kg^{-1} (not grouped) of MAP, BIO18, BIO4, AI, BIO15, and TP, respectively. Circle size indicates number of field plots. Black line is fitted linear effect; gray shading shows 95% confidence intervals; blue line is LOESS smooth line representing trend in MAP, BIO18, BIO4, AI, BIO15, and TP and responses of total C density, respectively. Red dots (n=149) represent measured value of total C density of forest ecosystems at different sites across the Greater Khingan Mountains with corresponding measured values of MAP, BIO18, BIO4, AI, BIO15, and TP, respectively.

References cited in the Supplementary Information

Belaïd, F., Youssef, A. B. & Lazaric, N. (2020). Scrutinizing the direct rebound effect for French households using quantile regression and data from an original survey. *Ecological Economics*, 176, 106755. https://doi.org/10.1016/j.ecolecon.2020.106755

Belward, A. S., Estes, J. E. & Kline, K. D. (1999). The IGBP-DIS global 1-km land-cover Data set discover: A project overview. *Photogrammetric engineering and remote sensing*, 65(9), 1013-1020.

Du, J., Tang, S. & Wang, H. (2000). Update models of forest resource data for subcompartments in natural forest. *Scientia Silvae Sinicae*, 36(2), 26-32 (in Chinese with English abstract).

Fang, L. & Yang, J. (2014). Atmospheric effects on the performance and threshold extrapolation of multi-temporal Landsat derived dNBR for burn severity assessment. *International Journal of Applied Earth Observation and Geoinformation*, 33, 10-20. https://doi.org/10.1016/j.jag.2014.04.017

Hai, L. (2009) *Studies on carbon sequestration of Larix gmelinii virgin forest and restoration forest after cutting*. M.Sc. thesis (in Chinese with English abstract), Inner Mongolia Agricultural University, Hohhot, China.

Huang, D. (2011) *Biomass and carbon storage estimation of Larix gmelinii plantation in different forest age*. M.Sc. thesis (in Chinese with English abstract), Northeast Forestry University, Harbin, China.

Karandinos, M. G. (1976). Optimum Sample Size and Comments on Some Published Formulae. *Bulletin of the Entomological Society of America*, 22(4), 417-421. https://doi.org/10.1093/besa/22.4.417

Koenker, R. (2005). *Quantile Regression*. Cambridge: Cambridge University Press.

Koenker, R. (2018). quantreg: Quantile Regression. R package version 5.35. Retrieved from https://CRAN.R-project.org/package=quantreg

Koenker, R. & Bassett, J., G (1978). Regression quantiles. *Econometrica: Journal of the Economic Society*, 102, 231-243. https://doi.org/10.1016/j.energy.2016.02.025

Koenker, R., Ng, P. & Portnoy, S. (1994). Quantile smoothing splines. *Biometrika*, 81(4), 673-680. https://doi.org/10.1093/biomet/81.4.673

Köhl, M., Magnussen, S. S. & Marchetti, M. (2006). *Sampling methods, remote sensing and GIS multiresource forest inventory*. Berlin-Heidelberg, Germany: Springer-Verlag.

Loveland, T. R. & Belward, A. S. (1997). The International Geosphere Biosphere Programme Data and Information System global land cover data set (DISCover). *Acta Astronautica*, 41(4), 681-689. https://doi.org/10.1016/S0094-5765(98)00050-2

Miller, J. D., Knapp, E. E., Key, C. H., Skinner, C. N., Isbell, C. J., Creasy, R. M. & Sherlock, J. W. (2009). Calibration and validation of the relative differenced Normalized Burn Ratio (RdNBR) to three measures of fire severity in the Sierra Nevada and Klamath Mountains, California, USA. *Remote Sensing of Environment*, 113(3), 645-656. https://doi.org/10.1016/j.rse.2008.11.009

Miller, J. D. & Thode, A. E. (2007). Quantifying burn severity in a heterogeneous landscape with a relative version of the delta Normalized Burn Ratio (dNBR). *Remote Sensing of Environment*, 109(1), 66-80. https://doi.org/10.1016/j.rse.2006.12.006

Pan, Y., Luo, T., Birdsey, R., Hom, J. & Melillo, J. (2004). New Estimates of Carbon Storage and Sequestration in China'S Forests: Effects of Age–Class and Method On Inventory-Based Carbon Estimation. *Climatic Change*, 67(2), 211-236. https://doi.org/10.1007/s10584-004-2799-5

Qi, G. (2011) *Carbon pool and sequestration potential of larch plantations in Northeast China*. PhD thesis (in Chinese with English abstract), Institute of Applied Ecology, CAS, Shenyang, China.

Qi, G., Wang, Q., Wang, X., Yu, D., Zhou, L., Zhou, W., . . . Dai, L. (2013). Soil organic carbon storage in different aged Larix gmelinii plantations in Great Xing'an Mountains of Northeast China. *Chinese Journal of Applied Ecology*, 24(1), 10-16 (in Chinese with English abstract).

SFAPRC. (2011). *Technical regulations for inventory for forest management planning and design.* Retrieved from https://www.doc88.com/p-9962134492051.html

Song, X. & Li, j. (2007). *Sampling survey techniques*. Beijing, China: China Forestry Press.

Wang, F. (2013) *Research on the carbon density and carbon balance of Larix gmelinii forest*. PhD thesis (in Chinese with English abstract), Inner Mongolia Agricultural University, Hohhot, China.

Xu, L., He, N. & Yu, G. (2020). *A dataset of carbon density in Chinese terrestrial ecosystems (2010s)*. National Ecosystem Science Data Center. Retrieved from http://www.cnern.org.cn/data/meta?id=40579

Yu, K., Lu, Z. & Stander, J. (2003). Quantile regression: applications and current research areas. *Journal of the Royal Statistical Society: Series D (The Statistician)*, 52(3), 331-350. https://doi.org/10.1111/1467-9884.00363

Zhu, Z. & Woodcock, C. E. (2012). Object-based cloud and cloud shadow detection in Landsat imagery. *Remote Sensing of Environment*, 118, 83-94. https://doi.org/10.1016/j.rse.2011.10.028